

Supplementary Information

Revisiting Carbazole-Based Polymer Donors for Efficient and Thermally Stable Polymer Solar Cells: Structural Utility of Coplanar π -Bridged Spacers

Geon-U Kim^{†,a}, Ji-Hyun Park^{†,b}, Seungjin Lee^a, Dongchan Lee^c, Jin-Woo Lee^a, Dahyun Jeong^a, Tan Ngoc-Lan Phan^a, Felix Sunjoo Kim^d, Shinuk Cho^c, Soon-Ki Kwon^{e,}, Yun-Hi Kim^{b,*}, and Bumjoon J. Kim^{a,*}*

^a Department of Chemical and Biomolecular Engineering, Korea Advanced Institute of Science and Technology (KAIST), Daejeon 34141, Republic of Korea

^b Department of Chemistry and RIGET, Gyeongsang National University, Jinju 52828, Republic of Korea

^c Department of Physics and EHSRC, University of Ulsan, Ulsan 44610, Republic of Korea

^d School of Chemical Engineering and Materials Science, Chung-Ang University (CAU), Seoul 06974, Republic of Korea

^e Department of Materials Engineering and Convergence Technology and ERI, Gyeongsang National University, Jinju 52828, Republic of Korea

*Corresponding author. *E-mail address:* skwon@gnu.ac.kr (S.-K. Kwon), ykim@gnu.ac.kr (Y.-H. Kim), bumjoonkim@kaist.ac.kr (B. J. Kim)

Table of Contents

Experimental Section

Supplementary Fig.s

- **Scheme S1.** Synthetic scheme for P1, P2, and P3.
- **Fig. S1.** ^1H -NMR and ^{13}C -NMR spectra of 4,8-bis(5-bromothiophen-2-yl)-6-(2-decyltetradecyl)-6*H*-bis([1,2,5]thiadiazolo)[3,4-*c*:3',4'-*g*]carbazole.
- **Fig. S2.** FAB Mass data of 4,8-bis(5-bromothiophen-2-yl)-6-(2-decyltetradecyl)-6*H*-bis([1,2,5]thiadiazolo)[3,4-*c*:3',4'-*g*]carbazole.
- **Fig. S3.** ^1H -NMR and ^{13}C -NMR spectra of 4,8-bis(5-bromo-6-nonylthieno[3,2-*b*]thiophen-2-yl)-6-(2-hexyldecyl)-6*H*-bis([1,2,5]thiadiazolo)[3,4-*c*:3',4'-*g*]carbazole.
- **Fig. S4.** FAB Mass data of 4,8-bis(5-bromo-6-nonylthieno[3,2-*b*]thiophen-2-yl)-6-(2-hexyldecyl)-6*H*-bis([1,2,5]thiadiazolo)[3,4-*c*:3',4'-*g*]carbazole.
- **Fig. S5.** ^1H -NMR and ^{13}C -NMR spectra of 4,8-bis(5-bromo-6-undecylthieno[3,2-*b*]thiophen-2-yl)-6-(2-decyltetradecyl)-6*H*-bis([1,2,5]thiadiazolo)[3,4-*c*:3',4'-*g*]carbazole.
- **Fig. S6.** FAB Mass data of 4,8-bis(5-bromo-6-undecylthieno[3,2-*b*]thiophen-2-yl)-6-(2-decyltetradecyl)-6*H*-bis([1,2,5]thiadiazolo)[3,4-*c*:3',4'-*g*]carbazole.
- **Fig. S7.** ^1H NMR spectrum of P1.
- **Fig. S8.** ^1H NMR spectrum of P2.
- **Fig. S9.** ^1H NMR spectrum of P3.
- **Fig. S10.** CV curves measured from pristine films of a) P1, P2, and P3 and b) Y6 and ferrocene.
- **Fig. S11.** a) The absorption spectra of Cz-based P_{DS} in film state and b) absorption coefficients in solution (chloroform) state.
- **Fig. S12.** Solubility of the polymers (P1, P2, and P3) in CF, CB, and THF solvents.
- **Fig. S13.** TGA thermograms for P1, P2, and P3.
- **Fig. S14.** a) The first cooling cycle and b) the second heating cycle of the DSC curves of the Cz-based P_{DS} .
- **Fig. S15.** Density functional theory (DFT) calculation results of Cz-based P_{DS} .
- **Fig. S16.** The current–voltage curves of hole-only devices.
- **Fig. S17.** Bandgap distributions of Cz-based P_{DS} :Y6 blend systems.
- **Fig. S18.** $V_{\text{oc}}^{\text{RadS}}$ of Cz-based P_{DS} :Y6 blends. Semi-logarithmic plots of FTPS-EQE (black line) and EL (blue line) as a function of energy. The pink line represents the ratio of ϕ_{EL} (EL photon flux) and ϕ_{BB} (black body spectrum), which corresponds to the reduced EQE spectrum.

- **Fig. S19.** EQE_{EEL} spectra of Cz-based P_{DS} :Y6 blends.
- **Fig. S20.** Light dependent characteristics of J_{sc} as a function of P from 0.01 to 1 Sun of Cz-based P_{DS} :Y6 blends.
- **Fig. S21.** The current–voltage curves from (a) hole-only and (b) electron-only devices of each blend.
- **Fig. S22.** AFM images of a) P1:Y6, b) P2:Y6, and c) P3:Y6 blend films.
- **Fig. S23.** a) 2D GIXS images of the Cz-based P_{DS} :Y6 blend films and Y6 pristine film and b) corresponding linecut profiles along the in-plane (q_{xy}) and out-of-plane (q_z) directions.
- **Fig. S24.** AFM height images of P1:Y6 and P3:Y6 blend films at 24 hr (a, c) and 144 hr (b, d) under 120 °C thermal annealing.
- **Fig. S25.** Phtostability of P1:Y6, P2:Y6, and P3:Y6-based PSCs.
- **Fig. S26.** a) Bandgap distributions, b) $V_{oc}^{Rad_s}$, and c) EQE_{EEL} spectra of P3:Y6:PC₇₁BM ternary blend system.

Supplementary Tables

- **Table S1.** GIXS information for the (100)_{IP} and (010)_{OOP} scattering peaks of Cz-based P_{DS} .
- **Table S2.** SCLC mobilities of the Cz-based P_{DS} pristine films.
- **Table S3.** Photovoltaic performances of P3:Y6 PSCs with different D/A ratios, additive volume fraction, and total concentrations.
- **Table S4.** ΔV_3 values of Cz-based P_{DS} :Y6 blends.
- **Table S5.** GIXS information for the (100)_{IP} and (010)_{OOP} scattering peaks of Cz-based P_{DS} :Y6.
- **Table S6.** Photovoltaic characteristics of the P1:Y6, P2:Y6, and P3:Y6 PSCs with annealing treatment at 120°C for different times.
- **Table S7.** ΔV_3 values of P3:Y6:PC₇₁BM blend.

References

Experimental Section

Materials

Y6, phenyl-C₇₁-butyric acid methyl ester (PC₇₁BM), and poly(3,4-ethylenedioxythiophene):poly(styrenesulfonate) (PEDOT:PSS) (Clevios P VP AI4083 and Heraeus Clevios PH1000) were purchased from Derthon, Nano-C, and Heraeus, respectively. Tetrakis(triphenylphosphine)palladium(0) (Pd(PPh₃)₄) was purchased from Umicore. Other chemicals and solvents were purchased from TCI, Alfa aesar, and Sigma Aldrich. The synthesis of 2,7-dibromo-dithiadiazole[3,4-*b*;7,8-*b'*]carbazole, tributyl(thiophen-2-yl)stannane, tributyl(6-undecylthieno[3,2-*b*]thiophen-2-yl)stannane, tributyl(6-nonylthieno[3,2-*b*]thiophen-2-yl)stannane, and 2,6-bis(trimethyltin)-4,8-bis(4-chloro-5-(2-ethylhexyl)thiophen-2-yl)benzo[1,2-*b*:4,5-*b'*]dithiophene were carried out using methods according to the previous literatures.¹⁻⁴

Synthesis

4,8-Dibromo-6-(2-hexyldecyl)-6H-bis([1,2,5]thiadiazolo)[3,4-*c*:3',4'-*g*]carbazole (1)

4,8-Dibromo-6H-bis([1,2,5]thiadiazolo)[3,4-*c*:3',4'-*g*]carbazole (4 g, 9.067 mmol), 7-(bromomethyl)pentadecane (4.15 g, 13.6 mmol), KI (0.15 g, 0.906 mmol), and K₂CO₃ (3.13 g, 22.667 mmol) were dissolved in DMF (40 mL) with degassing by nitrogen for 30 min. The reaction mixture was stirred for 6 hr at 90°C. After cooling to room temperature, the reaction mixture was extracted with ethyl acetate. The organic layer was washed with water and then dried over MgSO₄. After the solvent was evaporated, the crude product was purified by column chromatography (eluent = hexane/ ethyl acetate 10:1). After purification, the product was obtained as a yellow solid (yield: 3.65 g, 60.4%). ¹H NMR (300 MHz, CD₂Cl₂) δ = 7.93 (s, 2H), 4.21-4.19 (d, J=7.4Hz, 2H), 1.99-1.95 (m, 1H), 1.26-1.18 (m, 24H), 0.77-0.70 (m, 6H).

^{13}C NMR (500 MHz, CDCl_3): δ (ppm) = 151.0, 148.9, 137.7, 118.8, 111.5, 111.4, 49.0, 39.1, 31.8, 31.7, 31.5, 31.5, 29.7, 29.4, 29.4, 29.2, 26.3, 22.6, 14.0, 14.0; HRMS-FAB⁺ (m/z): calcd for $\text{C}_{28}\text{H}_{35}\text{Br}_2\text{N}_5\text{S}_2$ 663.0701, found 664.0773.

4,8-Dibromo-6-(2-decyltetradecyl)-6H-bis([1,2,5]thiadiazolo)[3,4-c:3',4'-g]carbazole (2)

4,8-Dibromo-6H-bis([1,2,5]thiadiazolo)[3,4-c:3',4'-g]carbazole (6 g, 13.6 mmol), 11-(bromomethyl)tricosane (8.5 g, 20.4 mmol), KI (0.22 g, 1.36 mmol), and K_2CO_3 (4.7 g, 34.004 mmol) were dissolved in *N,N*-dimethylformamide (DMF, 60 mL) with degassing by nitrogen for 30 min. The reaction mixture was stirred for 6 hr at 90°C. After cooling to room temperature, the reaction mixture was extracted with ethyl acetate. The organic layer was washed with water and then dried over MgSO_4 . After the solvent was evaporated, the crude product was purified by column chromatography (eluent = hexane/ ethyl acetate 10:1). After purification, the product was obtained as a yellow solid (yield: 6.6 g, 62.3%). ^1H NMR (300 MHz, CD_2Cl_2) δ = 7.92 (s, 2H) 4.22-4.19 (d, $J=7.7\text{Hz}$, 2H), 2.04 (s, 1H), 1.29-1.21 (m, 40H), 0.92-0.87 (m, 6H). ^{13}C NMR (500 MHz, CDCl_3): δ (ppm) = 151.1, 149.0, 137.8, 118.9, 111.6, 111.5, 49.1, 39.1, 31.9, 31.8, 31.5, 29.8, 29.6, 29.5, 29.5, 29.3, 29.2, 26.3, 22.6, 14.1; HRMS-FAB⁺ (m/z): calcd for $\text{C}_{36}\text{H}_{51}\text{Br}_2\text{N}_5\text{S}_2$ 775.1953, found 776.2054.

6-(2-Decyltetradecyl)-4,8-di(thiophen-2-yl)-6H-bis([1,2,5]thiadiazolo)[3,4-c:3',4'-g]carbazole (3)

4,8-Dibromo-6-(2-decyltetradecyl)-6H-bis([1,2,5]thiadiazolo)[3,4-c:3',4'-g]carbazole (1.9 g, 2.442 mmol), tributyl(thiophen-2-yl)stannane (3.64 g, 9.768 mmol) were dissolved in toluene (50 mL) with degassing by nitrogen for 30 min. $\text{Pd}(\text{PPh}_3)_4$ (0.14 g, 0.112 mmol) was added to the mixture, which was stirred for 10 hr at 120 °C. After cooling to room temperature, the reaction mixture was extracted with dichloromethane. The organic layer was washed with water and then dried over MgSO_4 . After the solvent was evaporated, the crude product was

purified by column chromatography (eluent = hexane/ dichloromethane = 1:1). After purification, the product was obtained as a orange solid (yield: 1.8 g, 93.9%). ¹H NMR (300 MHz, CD₂Cl₂) δ = 8.19-8.17 (dd, J=1.1 Hz, J=3.7 Hz, 2H), 7.92 (s, 2H), 7.54-7.52 (dd, J=1.0 Hz, J=5.1 Hz, 2H), 7.30-7.27 (dd, J=3.7 Hz, J=5.1 Hz, 2H), 4.31-4.28 (d, J=7.4 Hz, 2H), 2.10-2.06 (m, 1H), 1.42-1.20 (m, 40H), 0.90-0.89 (m, 6H). ¹³C NMR (500 MHz, CDCl₃): δ (ppm) = 150.7, 150.4, 139.9, 138.3, 128.1, 127.7, 126.4, 124.2, 112.1, 111.2, 48.5, 39.4, 31.9, 31.8, 29.8, 29.6, 29.5, 29.3, 29.3, 26.6, 22.7, 14.1; HRMS-FAB⁺ (m/z): calcd for C₄₄H₅₇N₅S₄ 783.3497, found 784.3586.

6-(2-Hexyldecyl)-4,8-bis(6-nonylthieno[3,2-b]thiophen-2-yl)-6H-bis([1,2,5]thiadiazolo)[3,4-c:3',4'-g]carbazole (4)

4,8-Dibromo-6-(2-hexyldecyl)-6H-bis([1,2,5]thiadiazolo)[3,4-c:3',4'-g]carbazole (2 g, 3.005 mmol), tributyl(6-nonylthieno[3,2-b]thiophen-2-yl)stannane (6.67 g, 12.02 mmol) were dissolved in toluene (50 mL) with degassing by nitrogen for 30 min. Pd(PPh₃)₄ (0.17 g, 0.1502 mmol) was added to the mixture, which was stirred for 10 hr at 120 °C. After cooling to room temperature, the reaction mixture was extracted with dichloromethane. The organic layer was washed with water and then dried over MgSO₄. After the solvent was evaporated, the crude product was purified by column chromatography (eluent = hexane/ dichloromethane = 1:1). After purification, the product was obtained as a orange solid (yield: 2.2 g, 70.6%). ¹H NMR (300 MHz, CD₂Cl₂) δ = 8.41 (s, 2H), 7.69 (s, 2H), 7.09 (s, 2H), 4.19-4.17 (d, J=7.4Hz, 2H), 2.81-2.76 (t, 4H), 2.01-2.00 (m, 1H), 1.90-1.80 (m, 4H), 1.45-1.18 (m, 48H), 0.96-0.91 (m, 6H), 0.86-0.80 (m, 6H). ¹³C NMR (500 MHz, CDCl₃): δ (ppm) = 150.3, 150.2, 140.2, 138.3, 138.2, 138.0, 134.2, 124.1, 120.6, 111.6, 111.3, 111.2, 39.6, 31.9, 31.9, 31.8, 29.8, 29.6, 29.5, 29.5, 29.4, 29.4, 29.3, 29.2, 29.2, 29.1, 26.8, 26.7, 22.7, 22.6, 14.1, 14.0; HRMS-FAB⁺ (m/z): calcd for C₅₈H₇₇N₅S₆ 1035.4503, found 1036.4565.

6-(2-Decyltetradecyl)-4,8-bis(6-undecylthieno[3,2-b]thiophen-2-yl)-6H-

bis([1,2,5]thiadiazolo)[3,4-c:3',4'-g]carbazole (5)

4,8-Dibromo-6-(2-decyltetradecyl)-6H-bis([1,2,5]thiadiazolo)[3,4-c:3',4'-g]carbazole (1.5 g, 1.928 mmol), tributyl(6-undecylthieno[3,2-b]thiophen-2-yl)stannane (4.49 g, 7.712 mmol) were dissolved in toluene (40 mL) with degassing by nitrogen for 30 min. Pd(PPh₃)₄ (0.11 g, 0.0964 mmol) was added to the mixture, which was stirred for 10 hr at 120°C. After cooling to room temperature, the reaction mixture was extracted with dichloromethane. The organic layer was washed with water and then dried over MgSO₄. After the solvent was evaporated, the crude product was purified by column chromatography (eluent = hexane/ dichloromethane = 1:1). After purification, the product was obtained as a orange solid (yield: 1.8 g, 77.4%). ¹H NMR (300 MHz, CD₂Cl₂) δ = 8.49 (s, 2H), 7.86 (s, 2H), 7.12 (s, 2H), 4.33-4.31 (d, J=7.4 Hz, 2H), 2.84-2.79 (t, 4H), 2.09-2.07 (m, 1H), 1.89-1.84 (m, 4H), 1.46-1.19 (m, 72H), 0.94-0.91 (m, 12H). ¹³C NMR (500 MHz, CDCl₃): δ (ppm) = 150.3, 150.2, 140.8, 139.6, 139.5, 138.1, 134.9, 124.3, 122.8, 121.2, 111.1, 111.0, 48.1, 39.5, 31.9, 31.8, 29.9, 29.9, 29.7, 29.6, 29.5, 29.5, 29.4, 29.3, 28.6, 26.8, 22.7, 14.1; HRMS-FAB⁺ (m/z): calcd for C₇₀H₁₀₁N₅S₆ 1203.6381, found 1204.6454.

4,8-Bis(5-bromothiophen-2-yl)-6-(2-decyltetradecyl)-6H-bis([1,2,5]thiadiazolo)[3,4-c:3',4'-g]carbazole (6)

6-(2-Decyltetradecyl)-4,8-di(thiophen-2-yl)-6H-bis([1,2,5]thiadiazolo)[3,4-c:3',4'-g]carbazole (1.8 g, 2.29 mmol), N-bromosuccinimide (NBS) (0.81 g, 4.58 mmol) were dissolved in tetrahydrofuran (THF, 40 mL) with degassing by nitrogen for 30 min. The reaction mixture was stirred for 4 hr at 25°C. The reaction mixture was extracted with dichloromethane. The organic layer was washed with water and then dried over MgSO₄. After the solvent was

evaporated, the crude product was purified by column chromatography (eluent = hexane/dichloromethane 1:1). After purification, the product was obtained as a red solid (yield: 1.85 g, 85.5%). ¹H NMR (300 MHz, CD₂Cl₂) δ = 7.78-7.76 (d, J=4.0 Hz, 2H), 7.63 (s, 2H), 7.19-7.18 (d, J=4.0 Hz, 2H), 4.14-4.11 (d, J=7.4 Hz, 2H), 1.98-1.95 (m, 1H), 1.32-1.20 (m, 40H), 0.93-0.88 (m, 6H). ¹³C NMR (500 MHz, CDCl₃): δ (ppm) = 150.3, 150.2, 141.1, 138.2, 130.7, 127.4, 123.3, 114.2, 111.3, 48.4, 39.4, 31.9, 31.8, 29.8, 29.6, 29.6, 29.3, 29.3, 26.7, 22.6, 14.1; HRMS-FAB⁺ (m/z): calcd for C₄₄H₅₅Br₂N₅S₄ 939.1707, found 940.1767.

4,8-Bis(5-bromo-6-nonylthieno[3,2-*b*]thiophen-2-yl)-6-(2-hexyldecyl)-6H-

bis([1,2,5]thiadiazolo)[3,4-*c*:3',4'-*g*]carbazole (7)

6-(2-Hexyldecyl)-4,8-bis(6-nonylthieno[3,2-*b*]thiophen-2-yl)-6H-bis([1,2,5]thiadiazolo)[3,4-*c*:3',4'-*g*]carbazole (2.0 g, 1.929 mmol), NBS (0.68 g, 3.858 mmol) were dissolved in THF (40 mL) with degassing by nitrogen for 30 min. The reaction mixture was stirred for 4 hr at 25°C. The reaction mixture was extracted with dichloromethane. The organic layer was washed with water and then dried over MgSO₄. After the solvent was evaporated, the crude product was purified by column chromatography (eluent = hexane/ dichloromethane 1:1). After purification, the product was obtained as a red solid (yield: 1.7 g, 73%). ¹H NMR (300 MHz, CD₂Cl₂) δ = 8.37 (s, 2H), 7.80 (s, 2H), 4.31-4.29 (d, J=7.4 Hz, 2H), 2.86-2.81 (t, 4H), 2.07-2.05 (m, 1H), 1.86-1.81 (m, 4H), 1.51-1.16 (m, 48H), 0.94-0.89 (m, 6H), 0.85-0.80 (m, 6H). ¹³C NMR (500 MHz, CDCl₃): δ (ppm) = 150.5, 150.4, 140.9, 139.7, 139.6, 138.3, 135.0, 124.6, 122.8, 121.3, 111.5, 111.2, 48.3, 39.6, 32.0, 31.9, 31.9, 31.8, 31.8, 29.9, 29.9, 29.6, 29.5, 29.5, 29.4, 29.3, 29.2, 28.6, 26.8, 26.7, 22.7, 22.6, 14.1; HRMS-FAB⁺ (m/z): calcd for C₅₈H₇₅Br₂N₅S₆ 1191.2713, found 1192.2795.

4,8-Bis(5-bromo-6-undecylthienof[3,2-*b*]thiophen-2-yl)-6-(2-decyltetradecyl)-6H-

bis([1,2,5]thiadiazolo)[3,4-*c*:3',4'-*g*]carbazole (8)

6-(2-Decyltetradecyl)-4,8-bis(6-undecylthieno[3,2-*b*]thiophen-2-yl)-6*H*-bis([1,2,5]thiadiazolo)[3,4-*c*:3',4'-*g*]carbazole (1.8 g, 1.493 mmol), NBS (0.53 g, 2.98 mmol) were dissolved in THF (40 mL) with degassing by nitrogen for 30 min. The reaction mixture was stirred for 4 hr at 25 °C. The reaction mixture was extracted with dichloromethane. The organic layer was washed with water and then dried over MgSO₄. After the solvent was evaporated, the crude product was purified by column chromatography (eluent = hexane/dichloromethane 1:1). After purification, the product was obtained as a red solid (yield: 1.7 g, 83.5%). ¹H NMR (300 MHz, CD₂Cl₂) δ = 8.30 (s, 2H), 7.64 (s, 2H), 4.18-4.16 (d, J=7.4Hz, 2H), 2.84-2.79 (t, 4H), 2.01-1.99 (m, 1H), 1.85-1.81 (m, 4H), 1.47-1.18 (m, 72H), 0.92-0.89 (m, 12H). ¹³C NMR (500 MHz, CDCl₃): δ (ppm) = 150.2, 150.1, 140.1, 138.1, 138.0, 137.9, 134.2, 123.9, 120.5, 111.6, 110.9, 110.8, 39.5, 31.9, 31.9, 29.9, 29.7, 29.7, 29.6, 29.6, 29.5, 29.4, 29.4, 29.3, 29.2, 28.1, 26.8, 22.7, 14.1; HRMS-FAB⁺ (m/z): calcd for C₇₀H₉₉Br₂N₅S₆ 1359.4591, found 1359.4581.

Polymerization of P1

In a 25 mL dry flask, 4,8-bis(5-bromothiophen-2-yl)-6-(2-decyltetradecyl)-6*H*-bis([1,2,5]thiadiazolo)[3,4-*c*:3',4'-*g*]carbazole (0.2000 g, 0.2123 mmol) and 2,6-bis(trimethyltin)-4,8-bis(4-chloro-5-(2-ethylhexyl)thiophen-2-yl)benzo[1,2-*b*:4,5-*b'*]dithiophene (0.2066 g, 0.2123 mmol) were dissolved in 8 mL toluene, then purged with nitrogen for 30 min. Pd(PPh₃)₄ (0.0122, 0.0106 mmol) was added to the mixture, which was stirred for 24 hr at 100°C under argon atmosphere. After cooling to room temperature, the reaction mixture was then dropped into methanol (200 mL). The crude polymer was collected by filtration and purified by Soxhlet extraction with methanol, acetone, hexane, and chloroform in sequence. The P1 was obtained by precipitation of the chloroform solution into methanol

(0.2 g, Yield: 64%). ^1H NMR (500 MHz, $\text{C}_2\text{D}_2\text{Cl}_4$) δ = 7.7-6.6 (broad, 10H), 3.2-2.8 (broad, 4H), 1.4-1.1 (broad, 79H).

Polymerization of P2

In a 25 mL dry flask, 4,8-bis(5-bromo-6-nonylthieno[3,2-*b*]thiophen-2-yl)-6-(2-hexyldecyl)-6*H*-bis([1,2,5]thiadiazolo)[3,4-*c*:3',4'-*g*]carbazole (0.2000 g, 0.1674 mmol) and 2,6-bis(trimethyltin)-4,8-bis(4-chloro-5-(2-ethylhexyl)thiophen-2-yl)benzo[1,2-*b*:4,5-*b'*]dithiophene (0.1629 g, 0.1674 mmol) were dissolved in 8 mL toluene, then purged with nitrogen for 30 min. $\text{Pd}(\text{PPh}_3)_4$ (0.0096 g, 0.00837 mmol) was added to the mixture, which was stirred for 24 hr at 100°C under argon atmosphere. After cooling to room temperature, the reaction mixture was then dropped into methanol (200 mL). The crude polymer was collected by filtration and purified by Soxhlet extraction with methanol, acetone, hexane, and chloroform in sequence. The P2 was obtained by precipitation of the chloroform solution into methanol (0.19 g, Yield: 70%). ^1H NMR (500 MHz, $\text{C}_2\text{D}_2\text{Cl}_4$) δ = 8.7-8.4 (broad, 2H), 7.8-7.0 (broad, 6H), 3.1-2.9 (broad, 6H), 1.5-0.8 (broad, 99H).

Polymerization of P3

In a 25 mL dry flask, 4,8-bis(5-bromo-6-undecylthieno[3,2-*b*]thiophen-2-yl)-6-(2-decyltetradecyl)-6*H*-bis([1,2,5]thiadiazolo)[3,4-*c*:3',4'-*g*]carbazole (0.2000 g, 0.1467 mmol) and 2,6-bis(trimethyltin)-4,8-bis(4-chloro-5-(2-ethylhexyl)thiophen-2-yl)benzo[1,2-*b*:4,5-*b'*]dithiophene (0.1428 g, 0.1467 mmol) were dissolved in 8 mL toluene, then purged with nitrogen for 30 min. $\text{Pd}(\text{PPh}_3)_4$ (0.0084 g, 0.0073 mmol) was added to the mixture, which was stirred for 24 hr at 100°C under argon atmosphere. After cooling to room temperature, the reaction mixture was then dropped into methanol (200 mL). The crude polymer was collected by filtration and purified by Soxhlet extraction with methanol, acetone, hexane, and chloroform in sequence. The P3 was obtained by precipitation of the chloroform solution into methanol

(0.19 g, Yield: 69%). ^1H NMR (500 MHz, $\text{C}_2\text{D}_2\text{Cl}_4$) δ = 8.7-8.3 (br, 2H), 7.8-6.8 (br, 6H), 3.4-2.8 (br, 6H), 1.4-0.8 (br, 123H).

Characterizations

The ^1H NMR and ^{13}C NMR spectra were recorded using a Bruker DRX 300 MHz and DRX 500 MHz spectrometer. The thermal analysis measurements were performed using a TA 2050 TGA thermogravimetric analyzer under nitrogen condition at a heating rate of $10\text{ }^\circ\text{C min}^{-1}$ from 0°C to 800°C . Differential scanning calorimetry (DSC) analysis was conducted under nitrogen at a heating $10\text{ }^\circ\text{C min}^{-1}$ from 0°C to 300°C using a TA Instruments 2100 DSC. UV-Vis absorption spectra were obtained using a Shimadzu's UV-3600. Absorption coefficients (ϵ_{film}) of thin films (as-cast using chloroform solvent) were calculated by dividing the absorbance by the film thickness of each material. Cyclic voltammetry (CV) was measured using a ZIVE SP1, Wonatech at room temperature in a 0.1 M solution of tetrabutylammonium percholate (Bu_4NClO_4) in chloroform. A three-electrode system was used, composing of a glassy carbon working electrode, a platinum wire counter electrode, and Ag/AgCl reference electrode. Size exclusion chromatography (Agilent GPC 1200), equipped with a refractive index detector (eluent: ortho-dichlorobenzene (o-DCB) at 80°C with polystyrene standards), was used to obtain the number-average molecular weight (M_n) and dispersity (\mathcal{D}) of polymers. External quantum efficiency (EQE) spectra were measured by K3100 IQX (McScience Inc.) and MC 2000 optical chopper (Thorlabs) under ambient conditions. To measure the morphologies/thicknesses of active layers, we used an atomic force microscopy (AFM, Parks Systems NX10). Grazing incidence X-ray scattering (GIXS) analysis was performed in the Pohang Accelerator Laboratory (beamline 9A, Republic of Korea), with incidence angle ($0.1^\circ - 0.14^\circ$). L_c values of the materials were calculated using Scherrer equation. $L_c = 2\pi K(\Delta q)^{-1}$,

where K (shape factor) = 0.9 and Δq is the full width at half maximum (FWHM) of the scattering peaks.

Space-charge-limited current (SCLC) mobility measurements

Hole (μ_h^{SCLC}) and electron mobilities (μ_e^{SCLC}) of pristine CZ-based P_{DS} and their blend films with Y6 were measured from SCLC method. For μ_h^{SCLC} values, hole-only devices with a device configuration of indium tin oxide (ITO)/PEDOT:PSS/pristine or blend films/Au were fabricated. For μ_e^{SCLC} values, electron-only devices with a structure of ITO/ZnO/blend films/Ca/Al were fabricated. The film thicknesses of the pristine and P_{DS} :Y6 blend films were in the range of 80 – 90 nm and 110 – 120 nm, respectively. The current–voltage characteristics were measured at the voltage range from 0 to 6 V, and corresponding results were fitted by the Mott-Gurney law:

$$J = \frac{9\varepsilon_0\varepsilon_r\mu_0V^2}{8L^3} \quad (1)$$

where J is the current density, ε_0 is the permittivity of free space (8.85×10^{-14} F cm⁻¹), ε_r is the relative dielectric constant of the transport medium (semi-conducting materials), μ_0 is the charge carrier (hole or electron) mobility, V is the effective applied voltage across the device ($V = V_{\text{applied}} - V_{\text{bi}} - V_r$, where V_{bi} is the built-in potential and V_r is the voltage drop caused by the resistance), and L is the thickness of the pristine or blend films. The hole and electron mobilities were calculated from the slope of the $J^{1/2}$ – V curves.

Fabrication of Polymer Solar Cells (PSCs)

The polymer solar cells (PSCs) were fabricated with a normal structure of ITO/PEDOT:PSS (AI4083)/active layers/PNDIT-F3N-Br/Ag. The ITO-coated glass substrates were ultra-sonicated using several cleaning solvents (acetone, deionized water, and isopropanol). Then, they were dried in the heating oven for 1hr. Next, for good wettability of AI4083, the cleaned ITO/glasses were treated with O₂ plasma for 10 min. As a hole transport layer, AI4083 was spin-coated at 3000 rpm onto the ITO/glass substrate and annealed at 165 °C for 15 min, and moved into a N₂-filled glovebox. For blending active layer of PX:Y6 (X=1, 2, and 3), chloroform (CF) was used as a processing solvent with a total concentration of 13 mg mL⁻¹ and a donor:acceptor (D:A) ratio of 1:1.2 w/w. To optimize the blend morphology, 1-chloronaphthalene (CN) of 0.7 vol% was added as a solvent additive and then stirred at 50°C for 2 hr. A P3:PC₇₁BM blend solution (D:A ratio of 1:1.5; total concentration of 22 mg mL⁻¹; solvent of chlorobenzene; additive of 1,8-diiodooctane 2 vol %) was prepared and heated at 70°C for 2 hr. For P3:Y6:PC₇₁BM ternary blend solution, D:A₁:A₂ ratio of 1:1.1:0.2, total concentration of 13 mg mL⁻¹, CF solvent, and 1-CN of 0.7 vol% were applied. Then, all the blend solutions were spin-coated for 40 s at 3000 rpm onto the HTL layer. After drying the active layers, PNDIT-F3N-Br solution (methanol, 1 mg mL⁻¹) as a electron transport layer was spin-coated at 3000 rpm, and finally, top electrode (Ag) of 120 nm was deposited through a thermal evaporator under high vacuum condition with ~10⁻⁶ Torr. For evaluating the performance of PSCs under light irradiation of 100 mW cm⁻², the current density–voltage (*J*–*V*) characteristics were obtained using Keithley 2400 SMU and K201 LAB55 solar simulator (McScience Inc.) with 150 W Xe short-arc lamp and filtered by an air mass 1.5G filter. To calibrate one-sun light intensity, a standard Si diode (the Class AAA, ASTM Standards) based on K801S-K302 Si reference cell (McScience Inc.) was used before each measurement. By optical microscopy, the active area of the PSC devices was measured to be 0.042 cm².

Measurement and calculation of bandgap (E_g^{PV}) and voltage loss (V_{loss})

Fourier-transform photocurrent spectroscopy (FTPS)-EQE measurements were performed by an INVENIO-R Fourier-transform infrared spectrometer, equipped with quartz beam splitter. To amplify the photo-current generated from PSCs under the illumination, a SR570 low-noise preamplifier from Stanford Research Systems was used and fed back into the external detector port of the FTIR. Electroluminescence (EL) signals were produced by using MAYA2000 PRO spectrophotometer from Ocean optics. The photovoltaic bandgap energy (E_g^{PV}) of Cz-based $P_{D5}:Y6$ blends was determined from the derivatives of the EQE spectra.^[2]

Calculation of voltage loss (V_{loss})

The voltage loss (V_{loss}) of PSCs is classified into three terms based on the detailed balance theory and reciprocity in solar cells:⁵

$$\begin{aligned} V_{loss} &= \Delta V_1 + \Delta V_2 + \Delta V_3 \\ &= (E_g^{PV}/q - V_{oc}^{SQ}) + (V_{oc}^{SQ} - V_{oc}^{Rad}) + (V_{oc}^{Rad} - V_{oc}^{PV}) \end{aligned} \quad (2)$$

1. The first V_{loss} term (ΔV_1) is defined by Shockley-Queisser (SQ) limit,⁶ and V_{oc}^{SQ} is calculated by below equation (3). where k_B is Boltzmann constant, T is temperature of PSCs, q is electric charge, $\phi_{AM\ 1.5G}$ is irradiance of standard solar simulator, and $\phi_{BB}(E)$ is the blackbody spectrum of semiconductor, given by equation (4):⁷, where h is Planck constant and c is speed of light.

$$V_{oc}^{SQ} = \frac{k_B T}{q} \ln \left[\frac{q \int_{E_g}^{\infty} \phi_{AM\ 1.5G}(E) dE}{q \int_{E_g}^{\infty} \phi_{BB}(E) dE} + 1 \right] \quad (3)$$

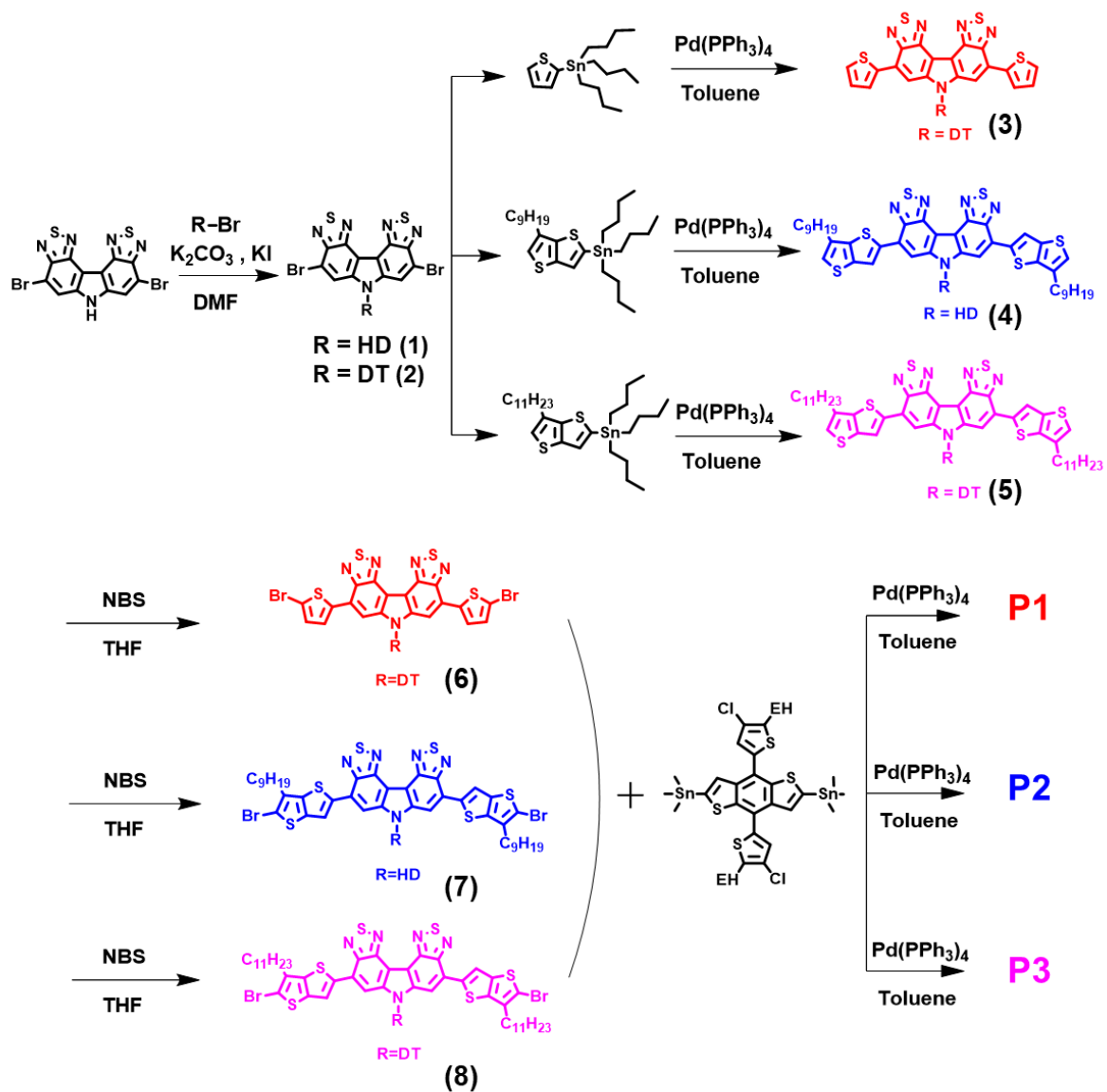
$$\phi_{BB}(E) = \frac{2\pi E^2}{h^3 c^2} \exp \left[-\frac{E}{k_B T} \right] \quad (4)$$

2. The second V_{loss} term (ΔV_2) is the offset between the SQ limited voltage and open-circuit voltage in the radiative limit ($V_{\text{oc}}^{\text{Rad}}$), where J_{sc} is short-circuit current density of solar cells and $Q_{\text{eqe}}(E)$ is the EQE obtained by the principle of detailed balance and reciprocity theorem.

$$V_{\text{oc}}^{\text{Rad}} = \frac{k_B T}{q} \ln \left[\frac{J_{\text{sc}}}{q \int_{E_g}^{\infty} Q_{\text{eqe}}(E) \cdot \phi_{\text{BB}}(E) dE} + 1 \right] \quad (5)$$

3. The third V_{loss} term (ΔV_3) is the non-radiative voltage loss, which is extracted by theoretical approach given by $\Delta V_3 = -\frac{k_B T}{q} \ln(\text{EQE}_{\text{EL}})$.⁸ Alternatively, ΔV_3 can be also obtained by subtracting the $V_{\text{oc}}^{\text{Rad}}$ from photovoltaic V_{oc} of PSCs.

Supplementary Scheme, Figures & Tables



Scheme S1. Synthetic scheme for P1, P2, and P3.

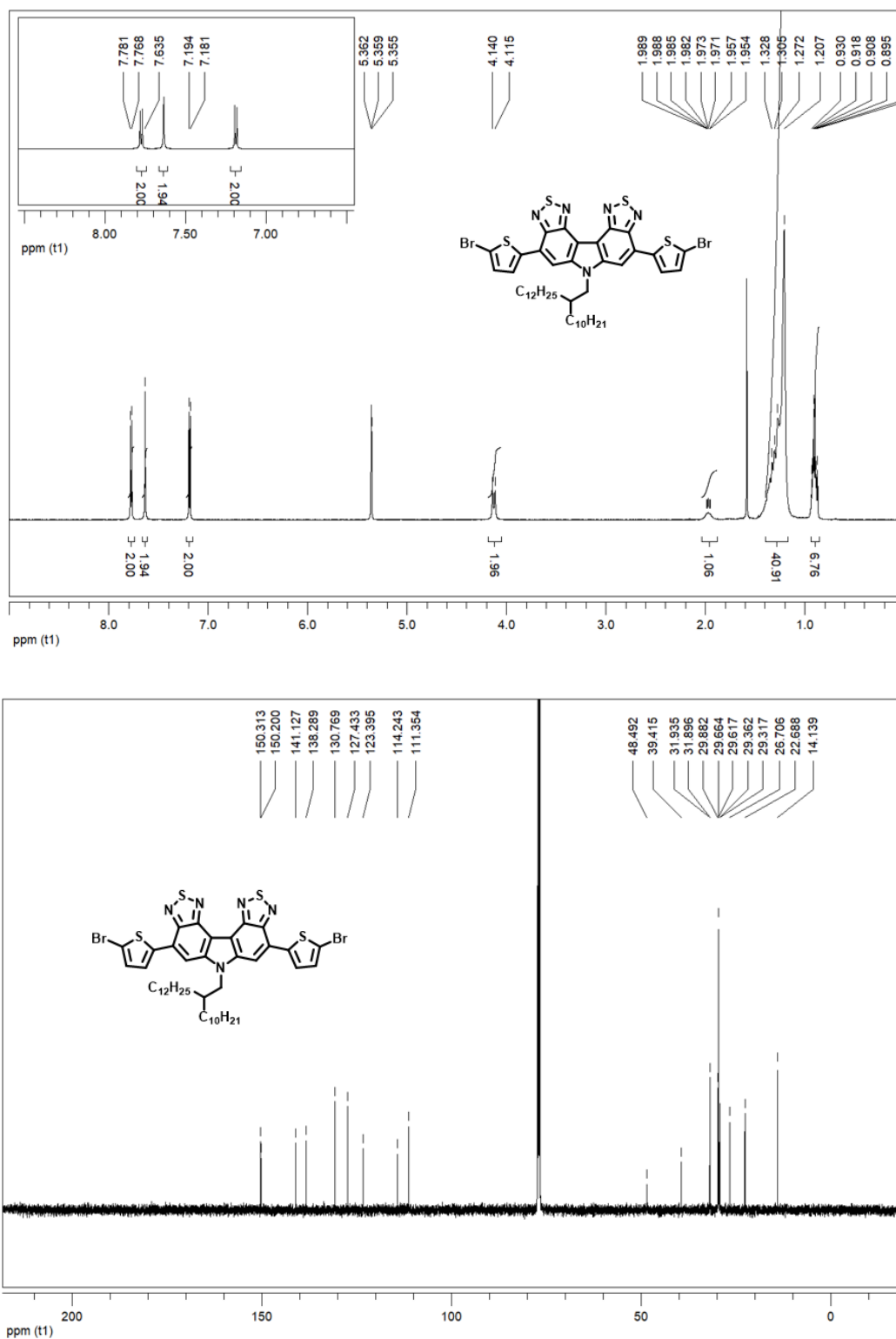


Fig. S1. ¹H-NMR and ¹³C-NMR spectra of 4,8-bis(5-bromothiophen-2-yl)-6-(2-decyltetradecyl)-6H-bis([1,2,5]thiadiazolo)[3,4-c:3',4'-g]carbazole.

[Mass Spectrum]
 Data : CBT-Th-Br-24 Date : 26-Feb-2021 17:21
 Inlet : Direct Ion Mode : FAB+
 RT : 0.64 min Scan# : 20

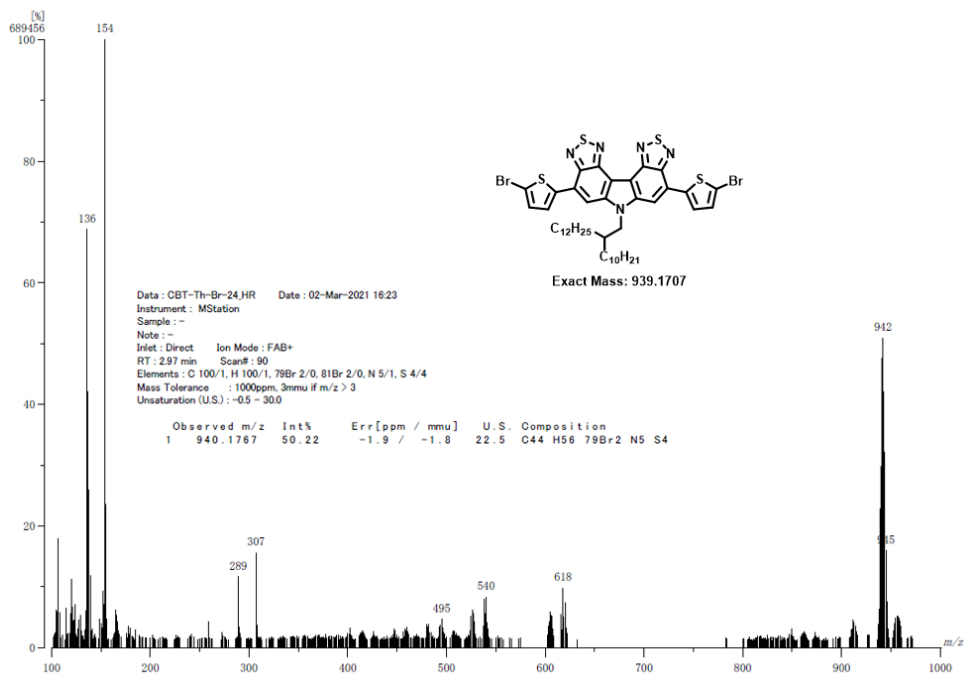


Fig. S2. FAB Mass data of 4,8-bis(5-bromothiophen-2-yl)-6-(2-decyltetradecyl)-6H-bis([1,2,5]thiadiazolo)[3,4-c:3',4'-g]carbazole.

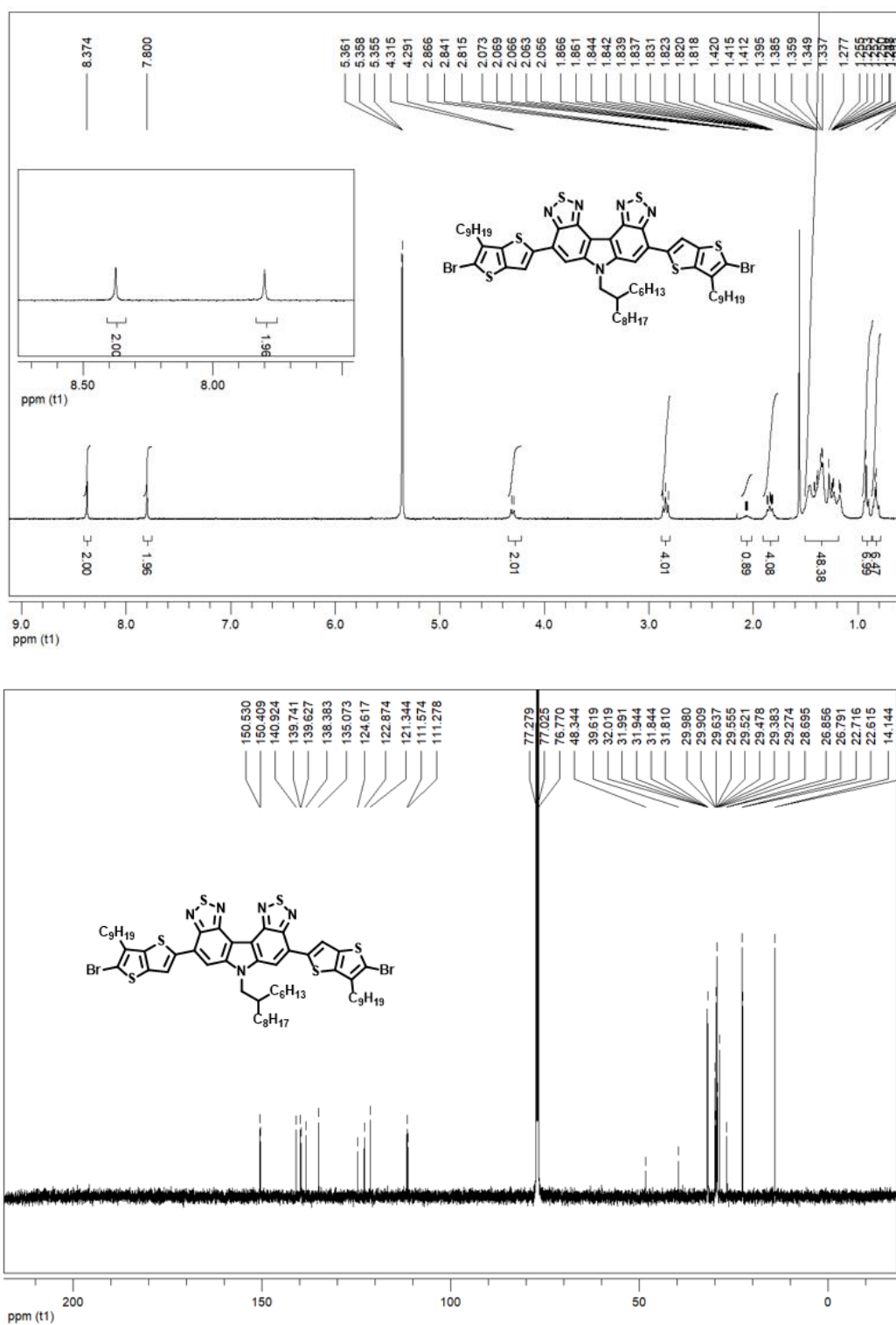


Fig. S3. ¹H-NMR and ¹³C-NMR spectra of 4,8-bis(5-bromo-6-nonylthieno[3,2-*b*]thiophen-2-yl)-6-(2-hexyldecyl)-6*H*-bis([1,2,5]thiadiazolo)[3,4-*c*:3',4'-*g*]carbazole.

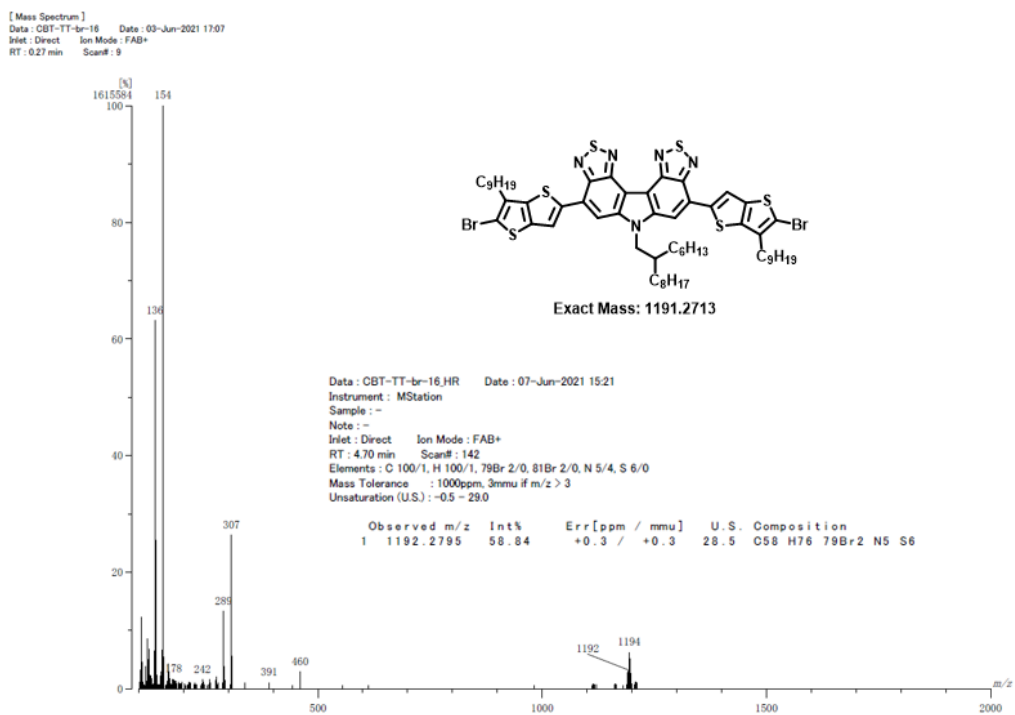


Fig. S4. FAB Mass data of 4,8-bis(5-bromo-6-nonylthieno[3,2-*b*]thiophen-2-yl)-6-(2-hexyldecyl)-6*H*-bis([1,2,5]thiadiazolo)[3,4-*c*:3',4'-*g*]carbazole.

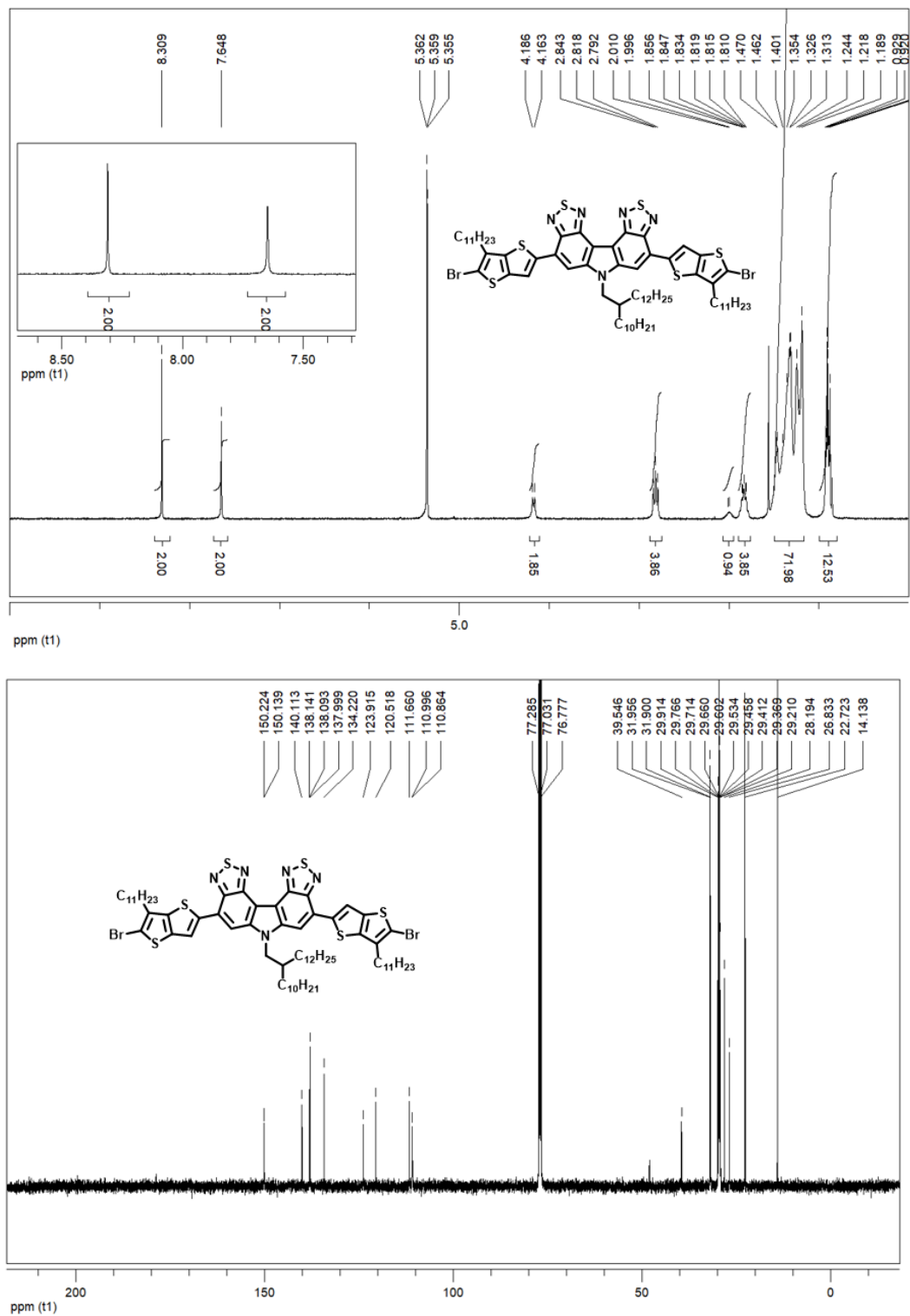


Fig. S5. ¹H-NMR and ¹³C-NMR spectra of 4,8-bis(5-bromo-6-undecylthieno[3,2-*b*]thiophen-2-yl)-6-(2-decyltetradecyl)-6*H*-bis([1,2,5]thiadiazolo)[3,4-*c*:3',4'-*g*]carbazole.

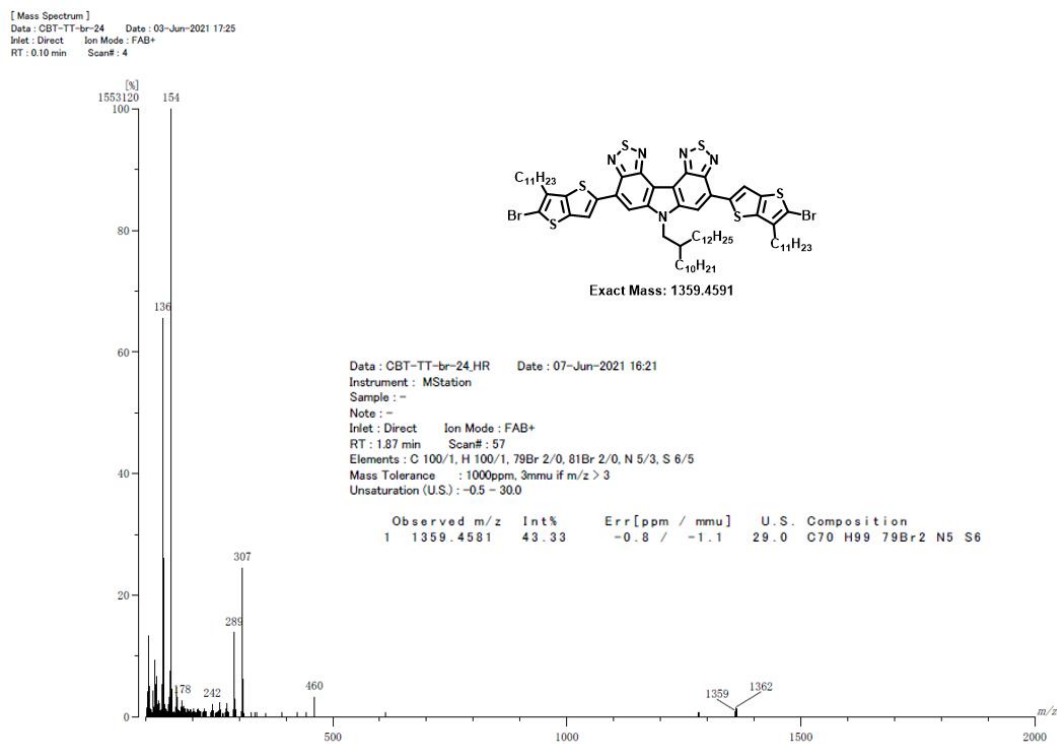


Fig. S6. FAB Mass data of 4,8-bis(5-bromo-6-undecylthieno[3,2-*b*]thiophen-2-yl)-6-(2-decyltetradecyl)-6*H*-bis([1,2,5]thiadiazolo)[3,4-*c*:3',4'-*g*]carbazole.

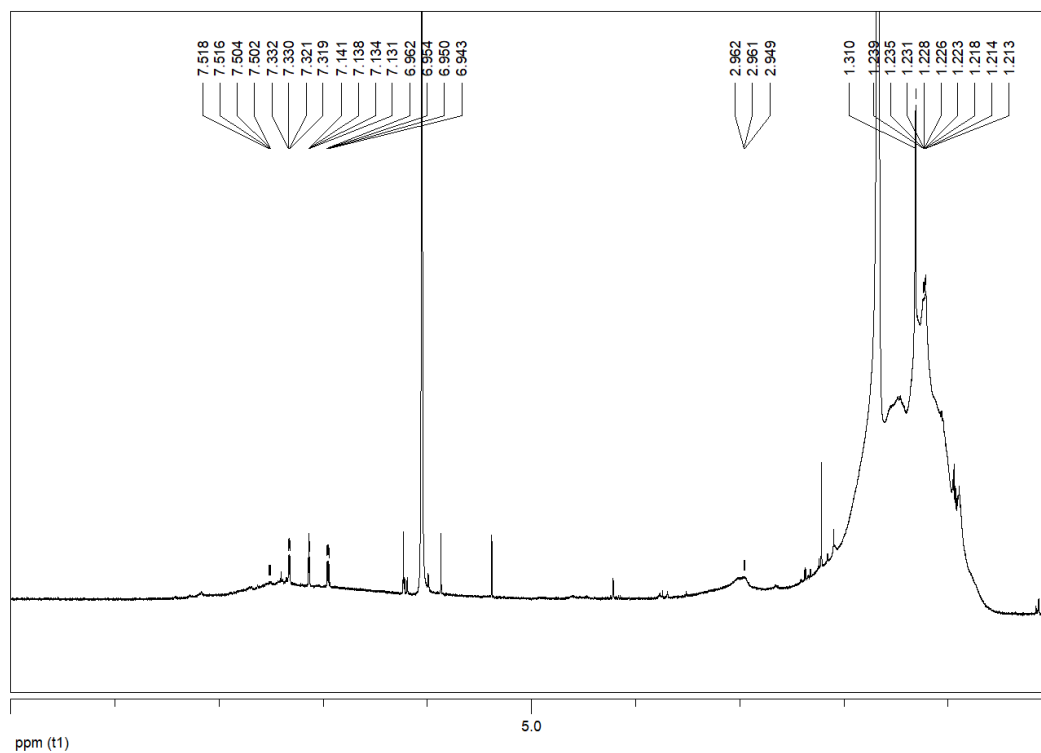


Fig. S7. ^1H NMR spectrum of P1.

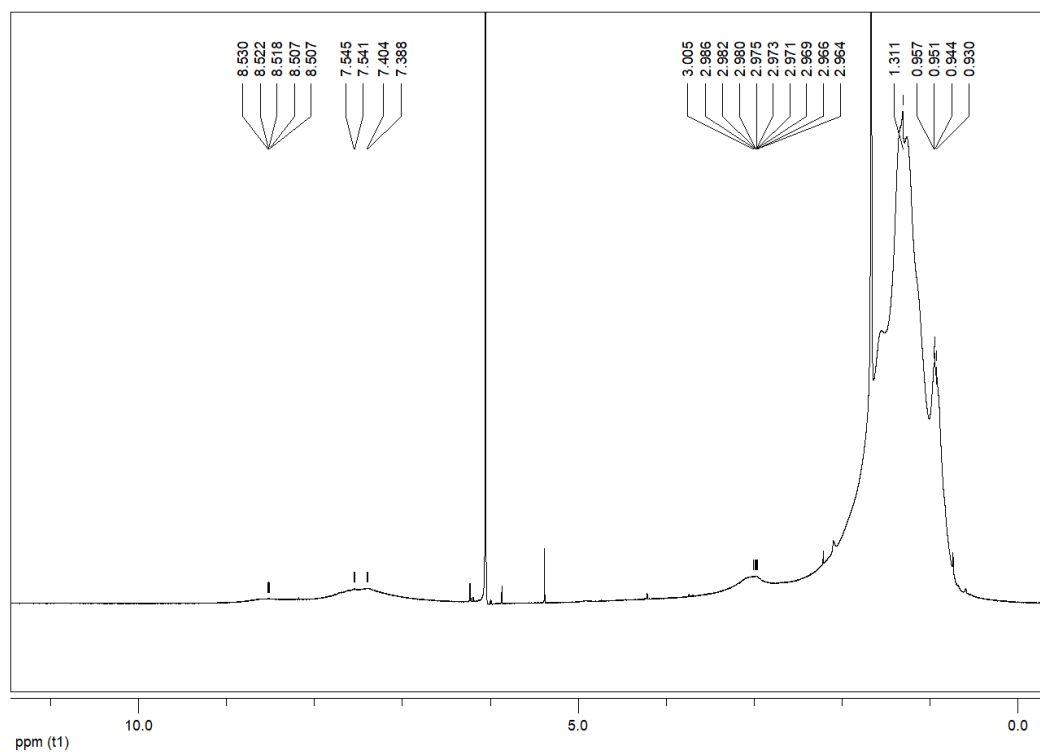


Fig. S8. ¹H NMR spectrum of P2.

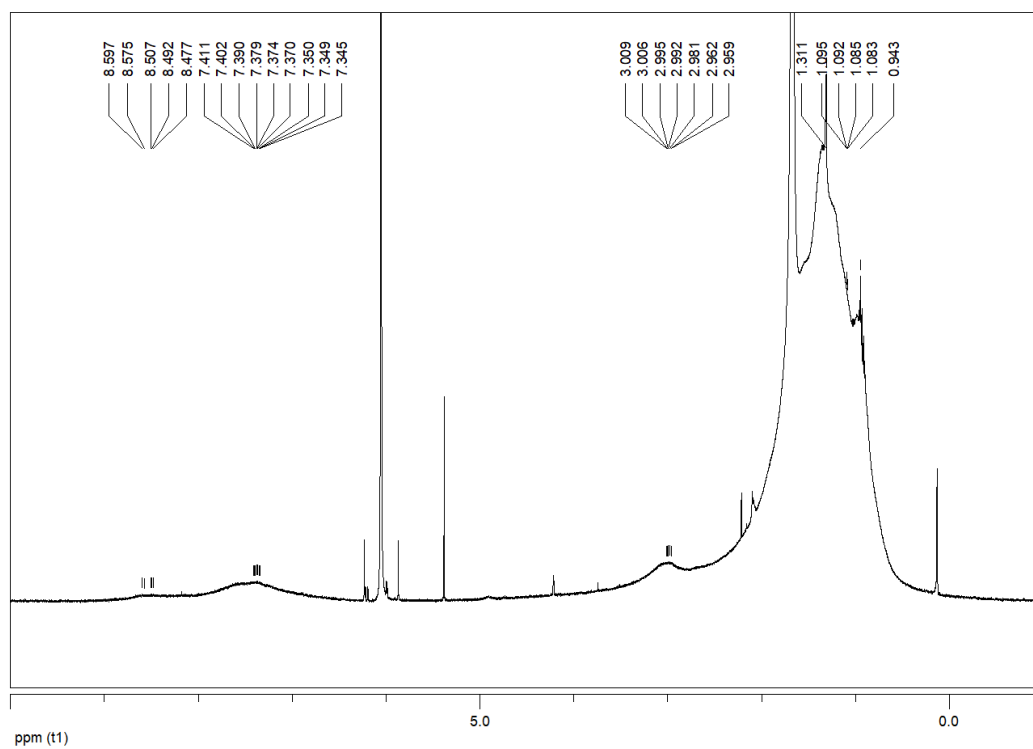


Fig. S9. ¹H NMR spectrum of P3.

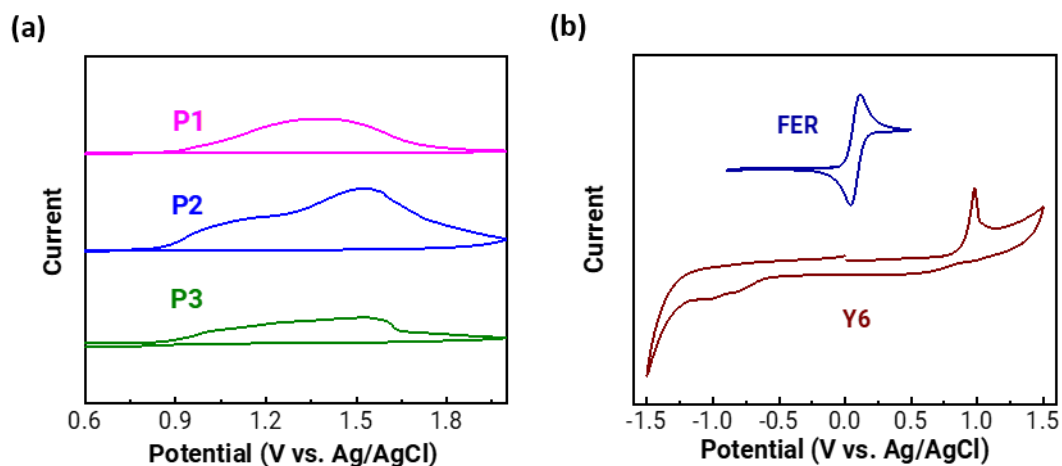


Fig. S10. CV curves measured from pristine films of a) P1, P2, P3, and b) Y6 and ferrocene.

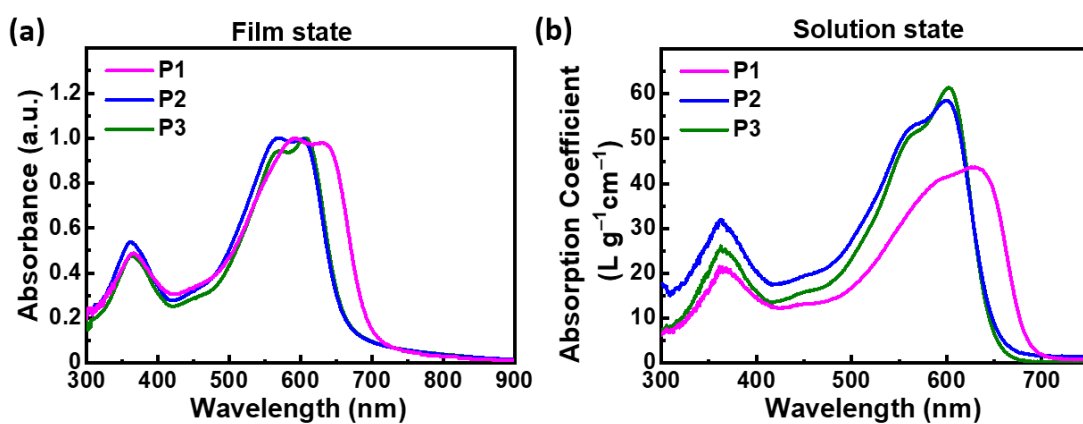


Fig. S11. a) The absorption spectra of Cz-based P_{DS} in film state and b) absorption coefficients in solution (chloroform) state.

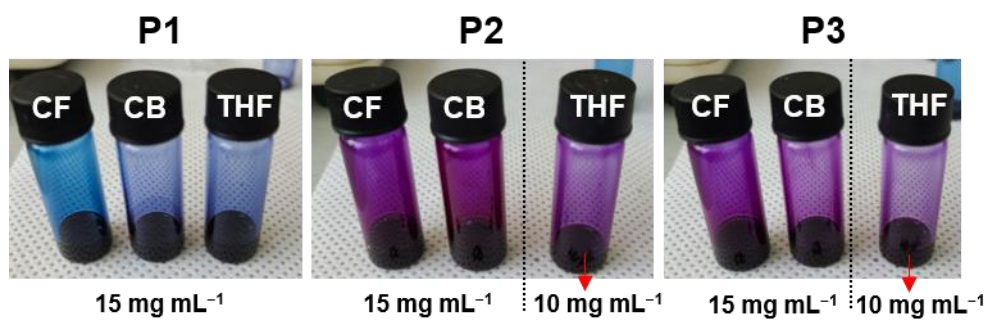


Fig. S12. Solubility of the polymers (P1, P2, and P3) in CF, CB, and THF solvents.

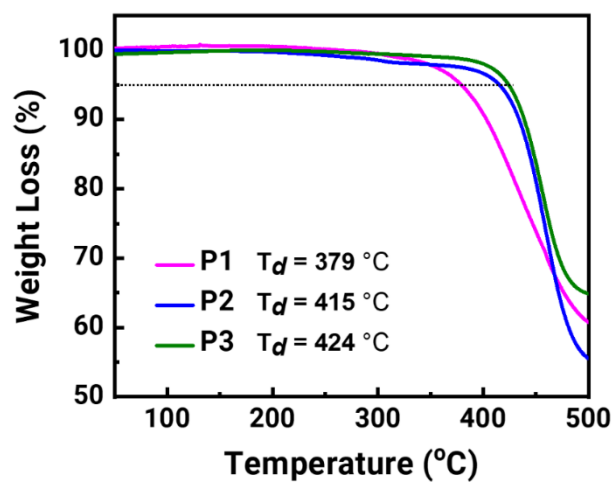


Fig. S13. TGA thermograms for P1, P2, and P3.

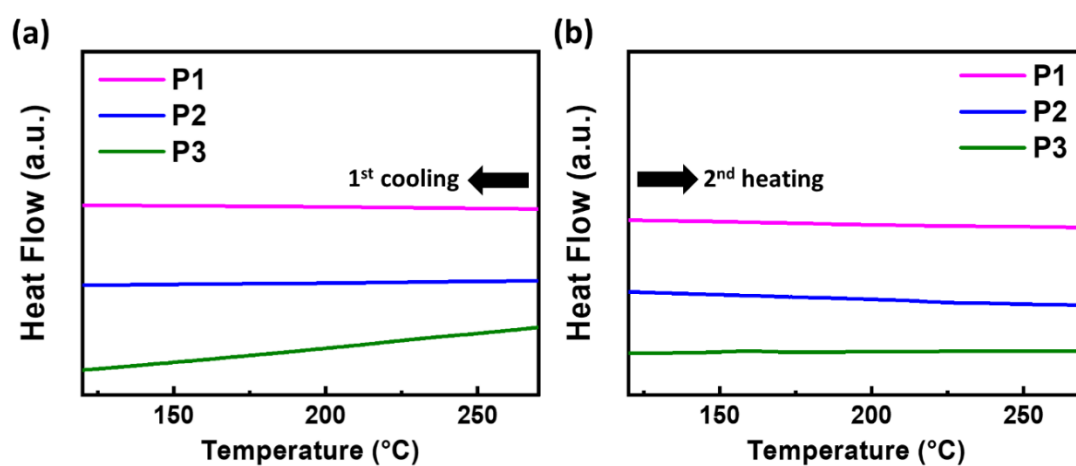


Fig. S14. a) The first cooling cycle and b) the second heating cycle of the DSC curves of the Cz-based P_{DS} .

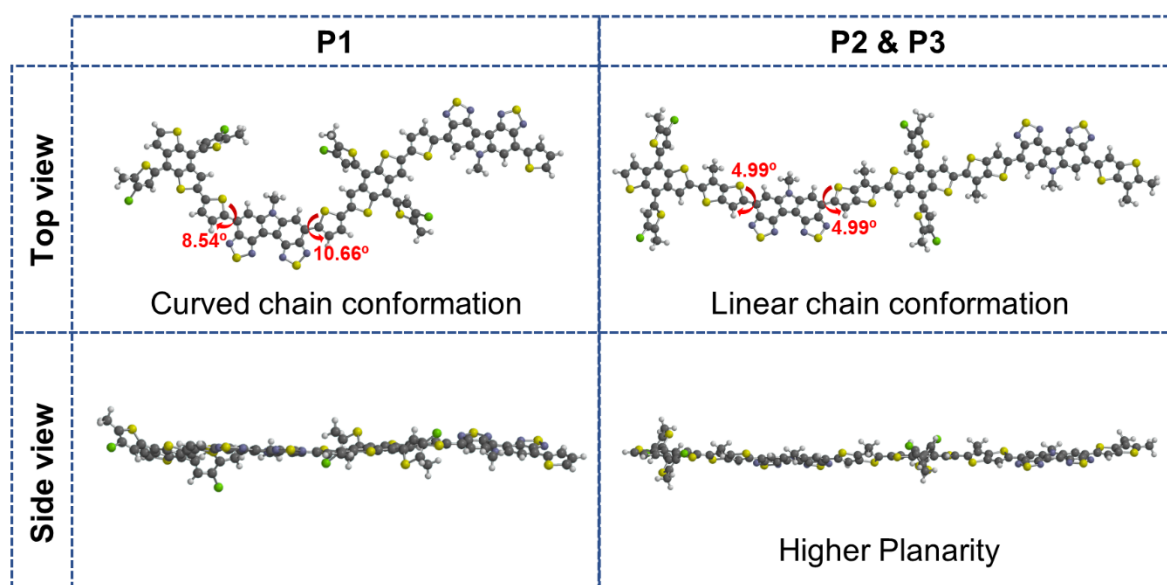


Fig. S15. Density functional theory (DFT) calculation results of Cz-based P_{DS} .

Table S1. GIXS information for the (100)_{IP} and (010)_{OOP} scattering peaks of Cz-based *P*_{DS}.

Pristine Film	q_{xy}	d -spacing	q_z	L_c	L_c
	(100) [Å ⁻¹]	(100) _{IP} [Å]	(010) [Å ⁻¹]	(100) _{IP} [nm]	(010) _{OOP} [nm]
P1	0.26	24.2	1.68	4.29	1.02
P2	0.28	22.4	1.61	4.51	1.83
P3	0.26	24.2	1.62	5.57	1.93

Table S2. SCLC mobilities of the Cz-based *P*_{DS} pristine films.

Pristine Film	μ_h^{SCLC} [cm ² V ⁻¹ s ⁻¹]
P1	8.24×10^{-5}
P2	1.65×10^{-4}
P3	2.05×10^{-4}

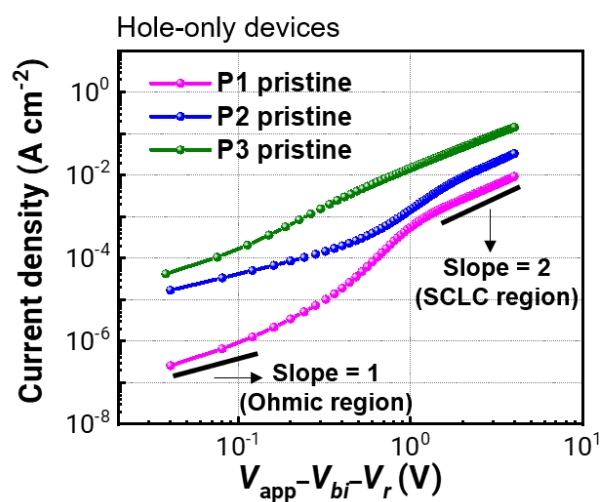
**Fig. S16.** The current–voltage curves of hole-only devices.

Table S3. Photovoltaic performances of P3:Y6 PSCs with different D:A ratios, additive volume fractions, and total concentrations.

D:A ratio [w/w]	Additive [CN, vol%]	Conc. [mg mL ⁻¹]	Annealing (100°C)	V_{oc} [V]	J_{sc} [mA cm ⁻²]	FF	PCE_{max} (PCE_{avg}) ^{a)} [%]
1:1				0.84	24.80	0.59	12.32 (11.89)
1:1.2	0.5	14	x	0.84	24.75	0.64	13.45 (12.99)
1:1.4				0.84	24.43	0.62	12.68 (12.45)
		12		0.84	24.07	0.66	13.25 (12.76)
1:1.2	0.5	13	x	0.85	24.57	0.67	13.99 (13.67)
		14		0.84	24.75	0.64	13.45 (12.99)
	0.5			0.85	24.57	0.67	13.99 (13.67)
1:1.2	0.7	13	x	0.84	24.37	0.70	14.32 (14.04)
	1.0			0.83	23.42	0.70	13.68 (13.58)
	2.0			0.83	22.85	0.66	12.57 (12.39)
1:1.2	0.7	13	7 min	0.83	24.66	0.71	14.58 (14.23)

^{a)}Active layers of the devices with a structure of ITO/PEDOT:PSS/active layer/PNDIT-F3N-Br/Ag were processed by chloroform. The average PCEs were determined from at least 15 devices.

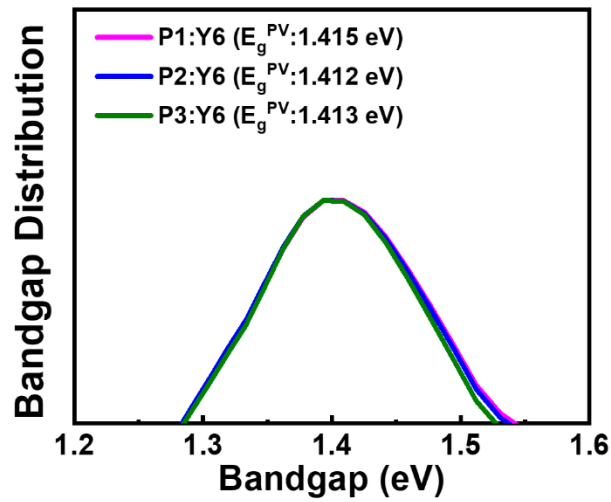


Fig. S17. Bandgap distributions of Cz-based P_{DS} :Y6 blend systems.

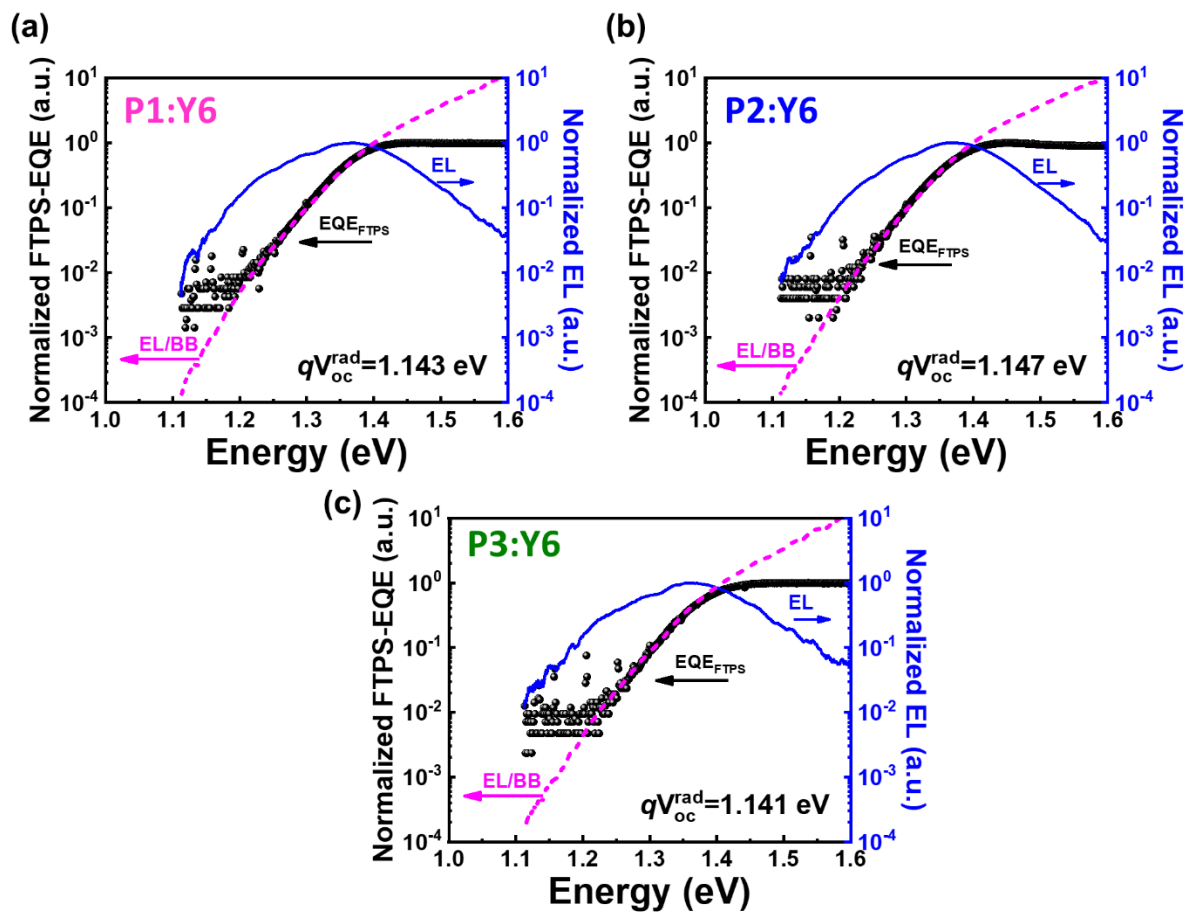


Fig. S18. V_{oc}^{rad} s of Cz-based P_{DS} :Y6 blends. Semi-logarithmic plots of FTPS-EQE (black line) and EL (blue line) as a function of energy. The pink line represents the ratio of ϕ_{EL} (EL photon flux) and ϕ_{BB} (black body spectrum), which corresponds to the reduced EQE spectrum.

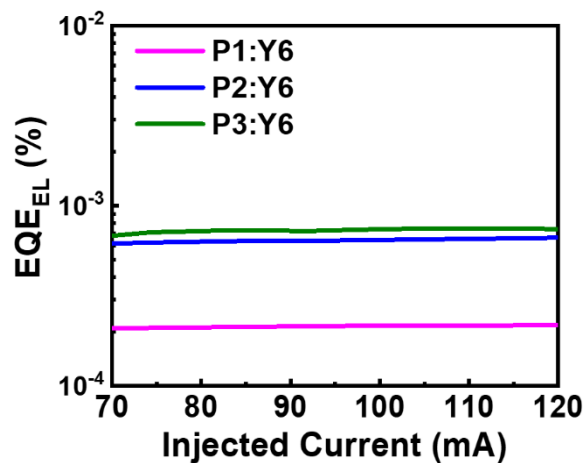


Fig. S19. EQE_{EL} spectra of Cz-based P_{DS} :Y6 blends.

Table S4. ΔV_3 values of Cz-based P_{DS} :Y6 blends.

Blend systems	ΔV_3 ^{a)}	ΔV_3 ^{b)}
P1:Y6	0.331	0.330
P2:Y6	0.310	0.307
P3:Y6	0.308	0.305

^{a)} Calculated by the equation: $\Delta V_3 = V_{\text{loss}} - \Delta V_1 - \Delta V_2$.

^{b)} Determined by the EQE_{EL} spectra.

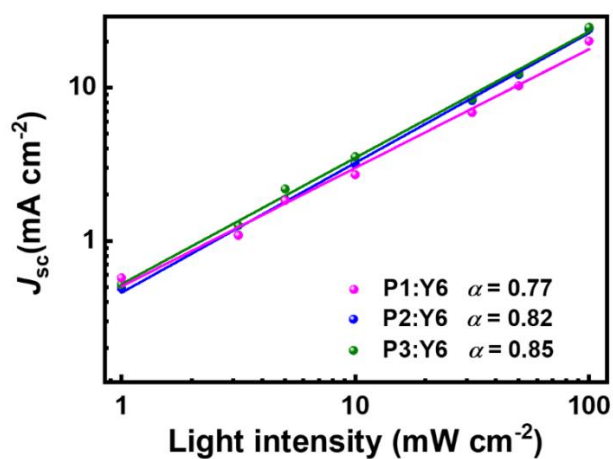


Fig. S20. Light dependent characteristics of J_{sc} as a function of P from 0.01 to 1 Sun of Cz-based P_{DS} :Y6 blends.

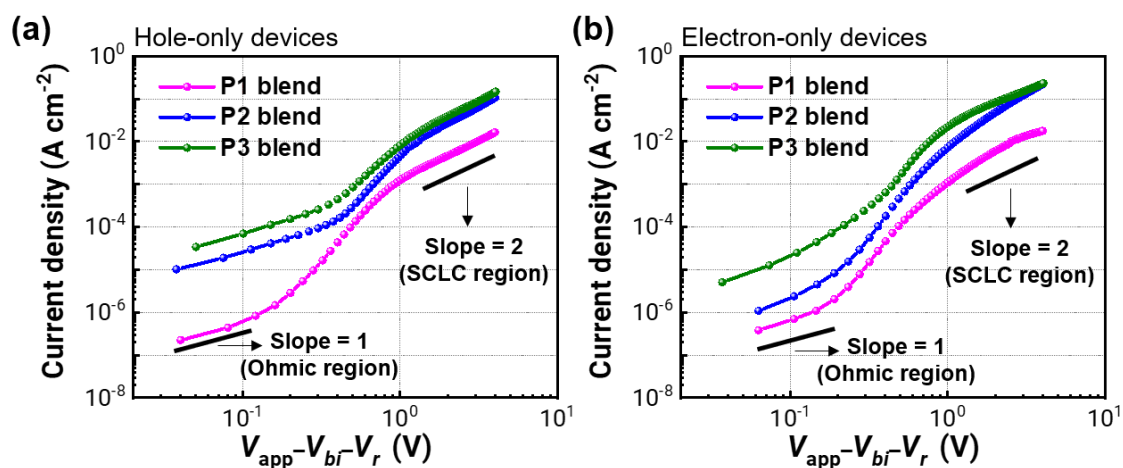


Fig. S21. The current–voltage curves from (a) hole-only and (b) electron-only devices of each blend.

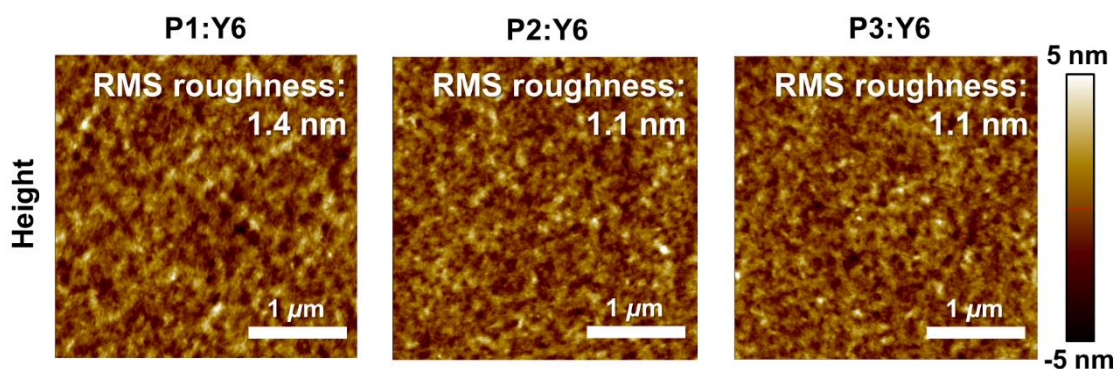


Fig. S22. AFM images of a) P1:Y6, b) P2:Y6, and c) P3:Y6 blend films.

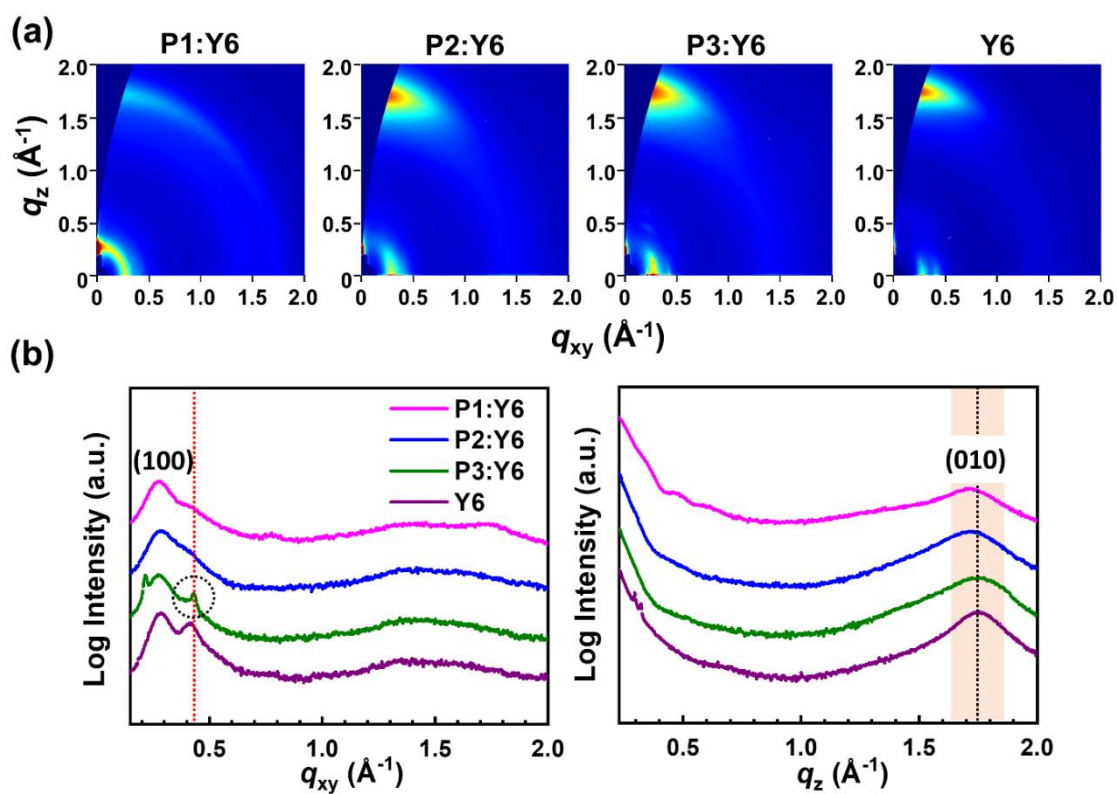


Fig. S23. a) 2D GIXS images of the Cz-based P_{DS} :Y6 blend films and Y6 pristine film and b) corresponding linecut profiles along the in-plane (q_{xy}) and out-of-plane (q_z) directions.

Table S5. GIXS information for the (100)_{IP} and (010)_{OOP} scattering peaks of Cz-based P_{DS}:Y6.

Film	q_{xy}	d -spacing	q_z	π - π distance
	(100) [Å ⁻¹]	(100) _{IP} [Å]	(010) [Å ⁻¹]	(010) _{OOP} [Å]
P1:Y6	0.28	22.4	1.71	3.67
P2:Y6	0.29	21.7	1.71	3.67
P3:Y6	0.28	22.4	1.74	3.61

Table S6. Photovoltaic characteristics of the P1:Y6, P2:Y6, and P3:Y6 PSCs with annealing treatment at 120°C for different times.

System	Time (hr)	V_{oc} (V)	J_{sc} (mA cm ⁻²)	FF	PCE _{max} (PCE _{avg}) ^a (%)
P1:Y6	0	0.80	22.22	0.61	10.75 (10.44 ± 0.33)
	24	0.70	19.94	0.51	7.15 (6.84 ± 0.31)
	48	0.65	18.13	0.48	5.66 (5.32 ± 0.38)
	96	0.65	17.45	0.46	5.24 (4.56 ± 0.89)
	144	0.66	17.64	0.45	5.17 (4.46 ± 0.98)
P2:Y6	0	0.84	24.08	0.65	13.17 (12.85 ± 0.31)
	24	0.81	24.39	0.62	12.31 (12.01 ± 0.29)
	48	0.80	24.71	0.59	11.63 (11.24 ± 0.36)
	96	0.80	23.92	0.60	11.48 (11.04 ± 0.42)
	144	0.79	23.85	0.59	11.17 (10.78 ± 0.40)
P3:Y6	0	0.84	24.37	0.70	14.32 (14.04 ± 0.27)
	24	0.79	25.55	0.69	13.77 (13.46 ± 0.30)
	48	0.79	25.19	0.68	13.56 (13.16 ± 0.38)
	96	0.79	24.90	0.69	13.44 (12.99 ± 0.43)
	144	0.78	24.03	0.68	12.91 (12.46 ± 0.48)

^a Average values and standard deviations were derived from more than 10 devices.

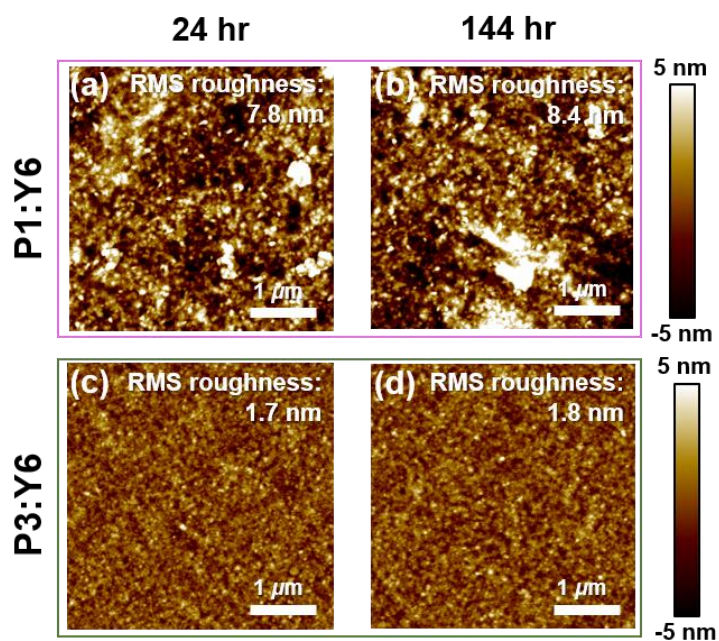


Fig. S24. AFM height images of P1:Y6 and P3:Y6 blend films at 24 hr (a, c) and 144 hr (b, d) under 120 °C thermal annealing.

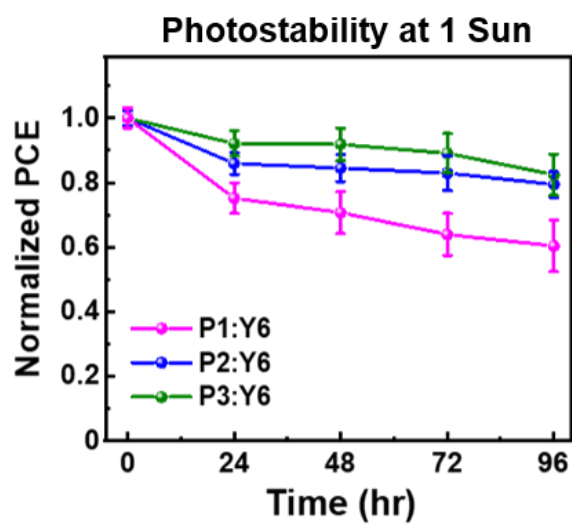


Fig. S25. Photostability of P1:Y6, P2:Y6, and P3:Y6-based PSCs.

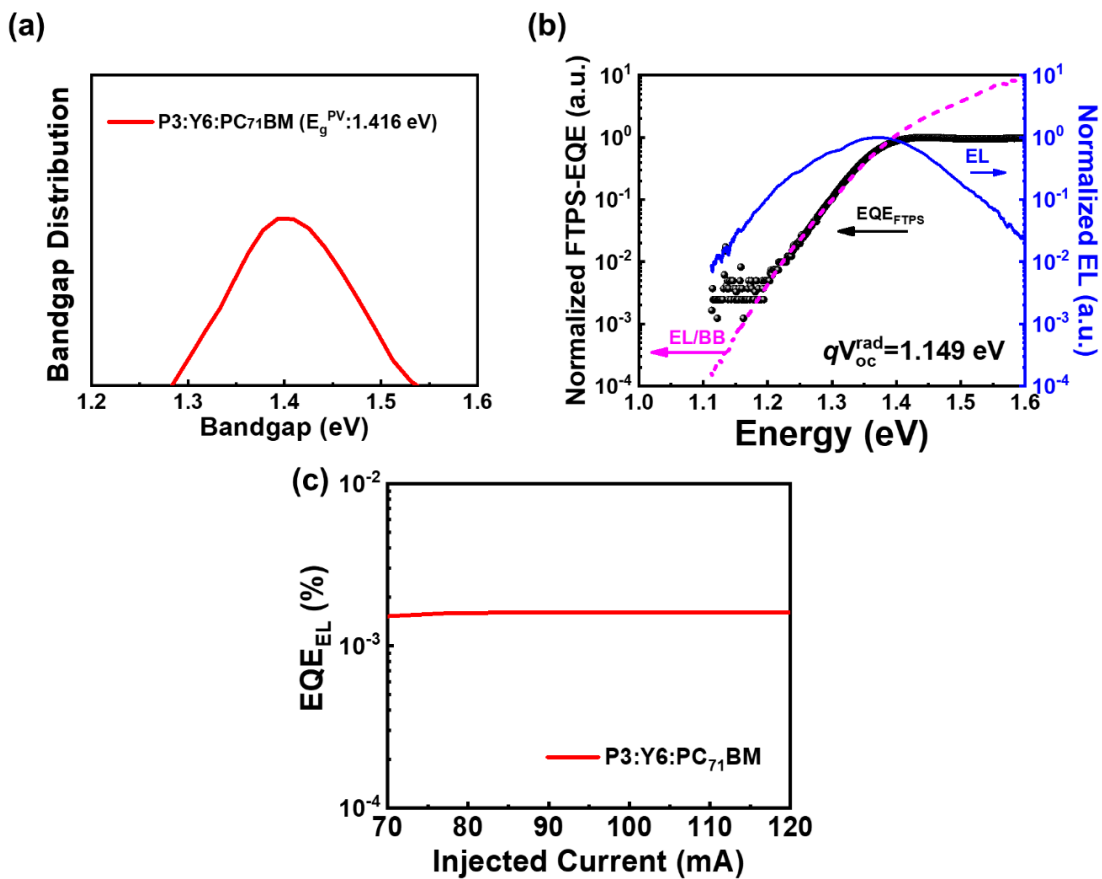


Fig. S26. a) Bandgap distributions, b) V_{oc}^{Rad} s, and c) EQE_{EL} spectra of P3:Y6:PC₇₁BM ternary blend system.

Table S7. ΔV_3 values of P3:Y6:PC₇₁BM blend.

Blend system	ΔV_3 ^{a)}	ΔV_3 ^{b)}
P3:Y6:PC ₇₁ BM	0.295	0.285

^{a)} Calculated by the equation: $\Delta V_3 = V_{loss} - \Delta V_1 - \Delta V_2$.

^{b)} Determined by the EQE_{EL} spectra.

References

1. P. Chao, Z. Mu, H. Wang, D. Mo, H. Chen, H. Meng, W. Chen and F. He, *ACS Appl. Energy Mater.*, 2018, **1**, 2365-2372.
2. J. Yu, T.-L. Shen, W.-H. Weng, Y.-C. Huang, C.-I. Huang, W.-F. Su, S.-P. Rwei, K.-C. Ho and L. Wang, *Adv. Energy Mater.*, 2012, **2**, 245-252.
3. D. Zha, L. Chen, F. Wu, H. Wang and Y. Chen, *J. Polym. Sci., Part A: Polym. Chem.*, 2013, **51**, 565-574.
4. X. Zhang, M. Köhler and A. J. Matzger, *Macromolecules*, 2004, **37**, 6306-6315.
5. U. Rau, B. Blank, T. C. M. Müller and T. Kirchartz, *Phys. Rev. Applied*, 2017, **7**, 044016.
6. W. Shockley and H. J. Queisser, *J. Appl. Phys.*, 1961, **32**, 510-519.
7. T. Kirchartz and U. Rau, *Phys. Status Solidi*, 2008, **205**, 2737-2751.
8. U. Rau, *Phys. Rev. B*, 2007, **76**, 085303.